JOURNAL OF THE AMERICAN WATER RESOURCES ASSOCIATION
DECEMBER AMERICAN WATER RESOURCES ASSOCIATION 2003

IMPACTS OF CALIFORNIA'S CLIMATIC REGIMES AND COASTAL LAND USE CHANGE ON STREAMFLOW CHARACTERISTICS[1]

R. Edward Beighley, John M. Melack, and Thomas Dunne[2]

ABSTRACT: To investigate the impacts of urbanization and climatic fluctuations on streamflow magnitude and variability in a Mediterranean climate, the HEC-HMS rainfall/runoff model is used to simulate streamflow for a 14-year period (October 1, 1988, to September 30, 2002) in the Atascadero Creek watershed located along the southern coast of California for 1929, 1998, and 2050 (estimated) land use conditions (8, 38 and 52 percent urban, respectively). The 14-year period experienced a range of climatic conditions caused mainly by El Niño-Southern Oscillation variations. A geographic information system is used to delineate the watershed and parameterize the model, which is calibrated using data from two streamflow and eight rainfall gauges. Urbanization is shown to increase peak discharges and runoff volume while decreasing streamflow variability. In all cases, the annual and 14-year distributions of streamflow are shown to be highly skewed, with the annual maximum 24 hours of discharge accounting for 22 to 52 percent of the annual runoff and the maximum ten days of discharge from an average El Niño year producing 10 to 15 percent of the total 14-year discharge. For the entire period of urbanization (1929 to 2050), the average increase in annual maximum discharges and runoff was 45 m^3/s (300 percent) and 15 cm (350 percent), respectively. Additionally, the projected increase in urbanization from 1998 to 2050 is half the increase from 1929 to 1998; however, increases in runoff (22 m^3/s and 7 cm) are similar for both scenarios because of the region's spatial development pattern.

(KEY TERMS: geographic information systems; land use change; rainfall/runoff modeling; streamflow variability; urbanization.)

Beighley, R. Edward, John M. Melack, and Thomas Dunne, 2003. Impacts of California's Climatic Regimes and Coastal Land Use Change on Streamflow Characteristics. Journal of the American Water Resources Association (JAWRA) 39(6):0000-0000.

INTRODUCTION

A Mediterranean climate is known for intense storms, which can give rise to sudden flooding (Ribolzi *et al.*, 2000). In southern California, mountainous coastal watersheds characteristically have thin soils on steep slopes, compounding the flooding impacts of intense rainfall. The effects of El Niño (unusually warm ocean temperatures in the equatorial Pacific typically producing above normal rainfall in southern California) and La Niña (unusually cold ocean temperatures typically producing below normal rainfall) on California's Mediterranean climate results in significant intra-annual and inter-annual variability in precipitation and flooding (Monteverdi and Null, 1997). While varying climatic conditions and resulting rainfall can be quantified, modeling the export of water from watersheds along the California south coast offers a variety of challenges. Pinol *et al.* (1997) note that modeling the hydrologic response in Mediterranean catchments is a particularly difficult problem because of the wetting up sequence following long, dry summers. Orographic enhancement of precipitation in the mountainous terrain further complicates the modeling challenge, especially when combined with the current upland development pattern in southern California's coastal watersheds. When development occurs in the headwaters rather than near the outlet, it tends to result in larger increases in peak discharge because more of the contributing drainage area responses are aligned by urbanization decreasing the time of concentration for areas most removed from the outlet, while maintaining the time of concentration for areas closest to the outlet (Beighley and Moglen, 2002). For example, if the headwaters of a watershed are developed, the runoff response from that area will likely reach the watershed outlet sooner than the response from the predeveloped conditions. If the response arrives at the

[1]Paper No. 03011 of the *Journal of the American Water Resources Association*. **Discussions are open until June 1, 2004.**

[2]Respectively, Post-Doc Researcher, Marine Science Institute, University of California, Santa Barbara, California 93106; and Professors, Bren School of Environmental Science and Management, Donald Bren Hall, University of California, Santa Barbara, California 93106-5131 (E-Mail/Beighley: beighley@icess.ucsb.edu).

watershed outlet sooner, it is more likely to coincide with peak responses from more downstream areas, resulting in an increase in the overall peak discharge at the outlet location.

Coastal watersheds also offer a variety of streamflow management challenges due to urbanization: increased flooding risk and severity and impaired water quality. In southern California, understanding the hydrologic impacts of coastal development is especially important because continued urbanization is predicted for the next 30 to 50 years (SBCPD, 2000; CADOF, 2001; Candau, 2002) and future climatic conditions may result in increased winter rainfall (Field *et al.*, 1999; McCarthy *et al.*, 2001; Kim *et al.*, 2002). Along the Santa Barbara coast, the coastal watersheds are bounded by the Pacific Ocean to the south and the Santa Ynez Mountains to the north (Figure 1) measuring 5 to 15 km from watershed divide to outlet. With development primarily confined to the coastal plain and foothills regions, approximately the lower half of a coastal watershed, city and county land use planners are tasked with accommodating future housing needs in a limited area. Understanding the hydrologic consequences (i.e., increased downstream flooding risk and severity) of future development can aid land use planners in allocating land for development and/or preservation.

Additionally, urbanization impacts the quantity and quality of streamflow entering the ocean. In southern California, understanding how changes in streamflow impact the nearshore ecosystem is important because giant kelp forests are located in the nearshore region and provide significant economic (i.e., kelp farming) and habitat resources. While kelp forests receive nutrients and organic material from numerous sources, understanding the terrestrial delivery mechanism, magnitude and variability of streamflow entering the ocean, will provide valuable insight for scientists focused on assessing the impacts of urbanization on kelp forest ecosystems. To provide land use planners and ecosystem scientists with an improved understanding of how urbanization and climate variability impact streamflow in southern California, this paper describes the effects of existing and future development on the magnitude and variability of annual and multiyear distributions of streamflow for a range of climatic conditions.

To meet this objective, an approach that integrates Geographic Information Systems (GIS) and hydrologic modeling was devised. A spatial/temporal database, consisting of both watershed and rainfall/runoff data, was developed and used to determine hydrologic modeling variables. These variables were then used to parameterize the HEC-HMS rainfall/runoff model

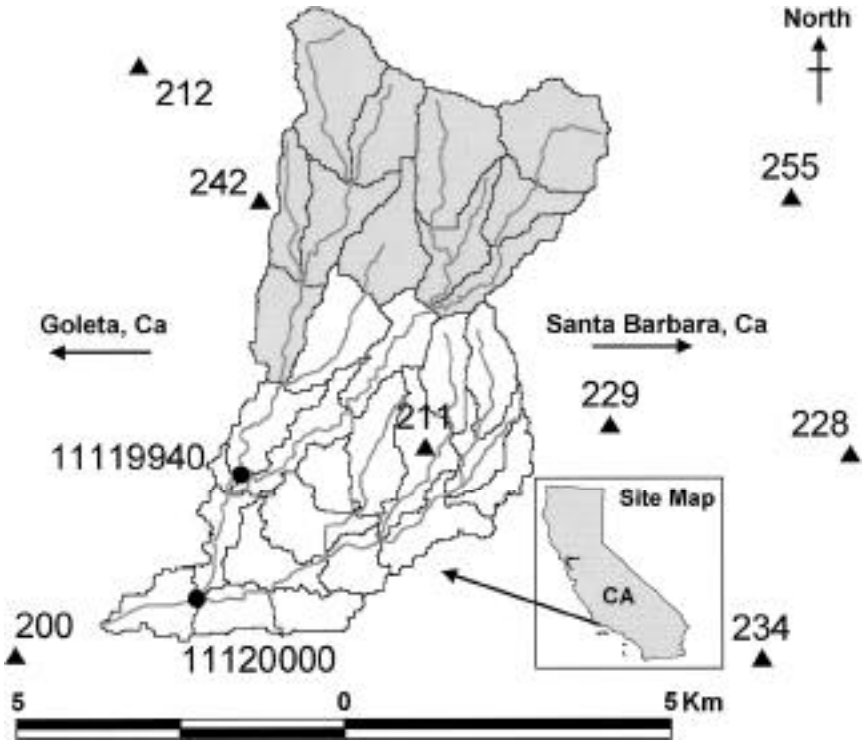

Figure 1. Atascadero Creek Watershed With Subarea Delineations, Stream Locations, Stream Gauges (circles), Precipitation Gauges (triangles), and Subareas Classified as Steep Shallow Soils (highlighted in gray).

(USACE, 2000). HEC-HMS is the U.S. Army Corps of Engineers' Hydrologic Modeling System (HMS) computer program developed by the Hydrologic Engineering Center (HEC). The model was calibrated and verified for current land use conditions and then used to simulate streamflow for two additional scenarios: historical conditions in 1929 representing predevelopment and projected urbanization in 2050 based on Candau (2002). Refer to the Alternative Land Use Scenarios section for details on 2050 land use projections. The three simulated streamflow series were then used to assess the effects of urbanization on annual and multiyear distributions of streamflow, peak discharges, and annual runoff for varying climatic conditions (i.e., El Niño and La Niña).

SITE DESCRIPTION

Atascadero Creek (50 km^2) drains the southern coast of California between Goleta and Santa Barbara (Figure 1) into the Goleta Slough and the Pacific Ocean (i.e., Santa Barbara Channel). The topography of the Atascadero Creek basin is representative of coastal watersheds draining into the Santa Barbara Channel from the Santa Ynez Mountains (approximately 50 coastal watersheds ranging in size from less than 10 km^2 to approximately 500 km^2), with mountainous headwaters and mild sloping coastal plains separated by transitional foothills. The Atascadero Creek watershed was selected for this study because it is currently undergoing urban development from both Goleta to the west and Santa Barbara to the east. There are two U.S. Geological Survey (USGS) stream gauges located within the watershed: (1) near the outlet, Gauge 11120000; and (2) at a main tributary, Gauge 11129940 (Figure 1). Table 1 provides gauging information and drainage area characteristics for these two gauges. The current watershed land use distribution is 38 percent urban (approximately 17 percent impervious), 51 percent shrub/brush, and 11 percent agricultural. In 1929, prior to major development, the watershed contained only 8 percent urban lands (about 4 percent impervious). It is predicted by Candau (2002) that the watershed will be 52 percent urban (24 percent impervious) in 2050, and the urban development, presently concentrated in the coastal plain, will extend upslope to mountainous lands.

The Mediterranean climate of the Atascadero Creek watershed supplies more than 80 percent of the annual rainfall in winter. The south sloping orientation of the watershed, the flow of moisture from the south-southwest during winter storms, and the steep mountainous terrain contribute to significant orographic precipitation (NOAA, 2001). Average annual precipitation over the past 40 years was approximately 50 cm (ranging from 20 to 120 cm) in the coastal plain and 85 cm (30 to 225 cm) in the mountains corresponding to an average annual watershed rainfall of 61 cm (ranging from 22 to 156 cm). Average annual watershed runoff over the past 60 years was approximately 10 cm (ranging from 0.1 to 53 cm). Most of the annual precipitation and corresponding runoff occurs in only a few large events, resulting in high peak discharges and a rapid return to near baseflow conditions. Thus, a large percentage of annual discharge occurs in 24 hours or less (Figure 2a). The period October 1, 1988, through September 30, 2002, was selected for this study because water year 1989 was the first year with both streamflow and rainfall data available at a temporal resolution of 15 minutes; high temporal resolution is required to model the rapid rainfall/runoff response in this region. The 14-year period is also representative of the expected range rainfall and runoff, with an average annual watershed rainfall and runoff of 65 cm (ranging from 21 to 145 cm) and 15 cm (ranging from 3 to 50 cm), respectively.

Regarding climate variability, Table 2 lists the climatic conditions: El Niño, La Niña, or normal, for each water year based on an analysis of ocean surface temperature in the tropical Pacific: high/low values of the Bivariate El Niño Southern Oscillation (ENSO) Timeseries "BEST" Index (Smith and Sardeshmukh, 2000). To illustrate the impact of these climatic conditions, Figure 2b shows the annual distribution of streamflow divided by the total 14-year discharge. The influence of El Niño conditions is evident, with

TABLE 1. USGS Stream Gauge Information. The mean daily flow is the long term average value for the period of record.

USGS ID	Creek Name	Area (km^2)	Relief (m)	Period of Record	Mean Daily Flow (m^3/s)
11119940	Maria Ygnacio	16.4	1,082	October 1, 1970, to Current	0.06
11120000	Atascadero	49.0	1,127	October 1, 1941, to Current	0.17

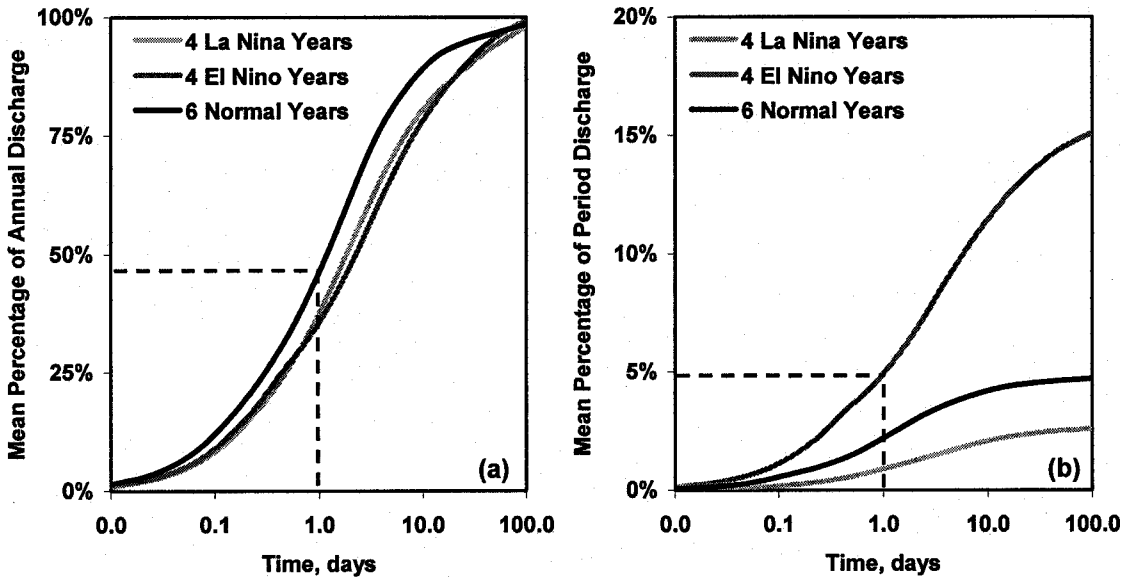

Figure 2. Mean Percentage of (a) Annual Discharge and (b) Total 14-Year Discharge, Exceeded in a Given Time Period for La Niña, El Niño, and Normal Years. The distributions for each water year were determined by cumulating the 15-minute discharges ranked in decreasing order and dividing by the (a) annual or (b) total 14-year discharge.

the maximum 10 days of discharge from an average El Niño year accounting for 12 percent of the total 14-year discharge compared to the maximum 10 days of flow from an average La Niña and normal year accounting for only 2 and 4 percent, respectively.

TABLE 2. Climatic Conditions; Runoff, Rainfall, and Runoff/ Rainfall Ratios for Water Years 1989 to 2002. Runoff is the simulated runoff at USGS Gauge 11120000 for 1998 land use and rainfall is based on Equation (4).

Water Year	Climatic Conditions	Runoff (cm)	Runoff (cm)	Runoff/ Rainfall (percent)
1989	La Niña	3.6	25.3	14.3
1990	Normal	2.9	21.3	13.4
1991	Normal	12.7	55.6	22.8
1992	El Niño	18.6	68.9	26.9
1993	El Niño	19.5	92.2	21.2
1994	Normal	7.0	47.0	15.0
1995	El Niño	50.1	144.7	34.6
1996	La Niña	11.2	60.6	18.4
1997	Normal	8.2	62.2	13.2
1998	El Niño	30.4	116.5	26.1
1999	La Niña	4.3	31.3	13.7
2000	La Niña	11.3	67.9	16.6
2001	Normal	23.1	89.7	25.8
2002	Normal	4.5	26.8	16.9

The annual runoff at the two USGS gauges ranges from 13 to 35 percent of the annual rainfall (Table 2). However, these annual ratios do not illustrate the intra-annual variability. For example, in 2001, the runoff/rainfall ratio was about 12 percent for a large rainstorm in January compared to nearly 50 percent for a similar storm in March. Generally, as the rainy season progresses and soil moisture increases, more runoff is produced for a given amount of rainfall.

MODEL DEVELOPMENT AND PARAMETERIZATION

The HEC-HMS rainfall/runoff model was used to simulate continuous streamflow for the Atascadero Creek watershed from October 1, 1988, to September 30, 2002, for three land use configurations: 1929, 1998, and 2050. HEC-HMS is a lumped parameter model, and the spatial pattern of development is incorporated into the model by subdividing the watershed into subareas that are approximately homogeneous in land use, soil type, slope, etc. HEC-HMS provides a suite of hydrologic modeling options for natural and engineered systems (USACE, 2000). The components used are described below.

Model Development

The Mediterranean climate and steep mountainous terrain affect storm runoff in several ways. There is a strong seasonal rainfall pattern, which affects initial watershed conditions. At the beginning of the rainy season, the catchments can accommodate a large amount of rainfall before producing a significant hydrograph response. As the rainy season progresses, runoff per unit of rainfall typically increases. Short, intense rainfalls are typical along the south coast (NOAA, 2001), so the temporal resolution of the model must be sufficient to preserve these intensities. The spatial distribution of rainfall in the model must capture the orographic enhancement. The geologic and topographic conditions indicate that the primary sources of subsurface storm flow are from shallow permeable soils on steep slopes over shaley bedrock and ground water flow from the deep permeable debris flow fans, alluvial fans, or coastal plains.

Based on our analysis of the regional hydrologic response, the HEC-HMS modeling options selected were: (1) the initial deficit constant loss infiltration routine, (2) kinematic wave routing for both overland and channel flow, and (3) exponential recession subsurface flow. The following discussion describes each modeling option. Refer to USACE (2000) for additional details. The initial deficit constant loss infiltration model was selected based on our observation that the initial conditions (i.e., initial storage capacity) and infiltration excess runoff (i.e., surface runoff only during intense rainfall) are dominant factors affecting the storm hydrographs. Additionally, this modeling framework can incorporate the effects of urbanization by increasing the percentage of impervious surface within a given subarea. Figure 3 illustrates our conceptual loss model. Our approach assumes that a subarea, *i*, has an initial and maximum storage capacity, and when precipitation begins, all rainfall not on impervious surfaces goes towards filling the initial deficit. Once the initial storage deficit is satisfied, runoff occurs if the rainfall rate exceeds the constant loss rate. It is assumed that all rainfall on impervious surfaces results in runoff. To summarize the loss model, the excess precipitation rate, $P_{e,i}(t)$ with units of length per time [L/T], from each subarea, *i*, is generated by

$$P_{e,i}(t) = \begin{cases} U_i P_i(t) & \text{for } S_i(t) < S_{m,i} \\ U_i P_i(t) + (1-U_i)(P_i(t) - I_i & \text{for } S_i(t) = S_{m,i} \text{ and } P_i(t) > I_i \\ U_i P_i(t) & \text{for } S_i(t) = S_{m,i} \text{ and } P_i(t) < I_i \end{cases} \quad (1)$$

where U_i is the percentage of impervious surface in subarea *i*; $P_i(t)$ [L/T] is precipitation rate; $S_i(t)$ [L] is the storage at time *t*; $S_{m,i}$ (L) is the maximum storage capacity; and I_i [L/T] is the constant loss rate. For continuous simulations, subarea storage is determined by

$$S_i(t) = \min | \; S_i(t-1) + (1 - U_i)P_i(t) - L_i(t) \text{ or } S_{m,i} \; | \quad (2)$$

where L_i (t) [L/T] is the storage reservoir recovery rate representing net losses such as evapotranspiration (ET) and deep ground water recharge (R). The recovery rate is adjusted monthly to simulate seasonal effects.

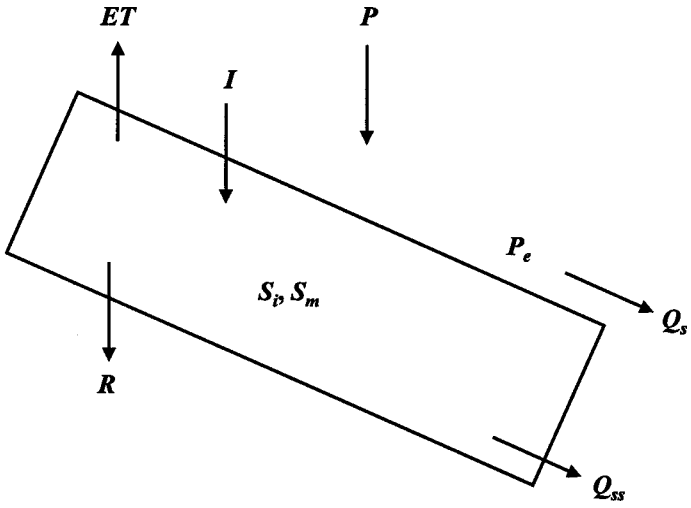

Figure 3. Rainfall/Runoff Model, Where *P* is Precipitation, P_e is Excess Precipitation, I is Infiltration, *ET* is Evapotranspiration, *R* is Deep Ground Water Recharge, S_i is the Storage at a Given Time Period, S_m is the Maximum Storage, Q_S is Surface Runoff, and Q_{SS} is Subsurface Runoff.

Kinematic wave routing was selected for both channel and overland flow because of the steepness of the watershed (Table 3). The kinematic wave method assumes subareas are large planes with a main channel that drains to the subarea outlet. The main channel receives lateral inflow from the overland flow

planes (i.e., $P_{e,i}(t)$), where overland flow is approximated as wide rectangular channel flow. For subareas with upstream inflow, the main channel routes the upstream flow as well as lateral inflow to the subarea outlet. The kinematic wave routing method requires shape, slope and roughness characteristics for both channel and overland components. To account for urbanization impacts on routing, overland and channel characteristics are modified to reflect altered land use conditions.

TABLE 3. Atascadero Creek Watershed Subarea Drainage Characteristics.

Subarea Parameters	Mean	Minimum	Maximum
Area (km^2)	1.6	0.2	3.3
Elevation (m)	236	11	897
Overland Slope (percent)	21.3	3.3	54.2
Overland Flow Length (km)	0.3	0.1	0.6
Channel Slope (percent)	16.1	3.0	39.1
Channel Flow Length (km)	2.8	1.2	4.3

The exponential recession model was selected to simulate subsurface response, determined by

$$Q_{ss,i}(t) = \max | \alpha \hat{Q}_i(t)\, k' - Q_{s,i}(t) \;\; or \;\; Q_{ss,i}(t-1) k^{\Delta t} | \tag{3}$$

where $Q_{ss,i}(t)$ [L^3/T] is the subsurface flow; $Q_{s,i}(t)$ [L^3/T] is surface flow at time t; $\hat{Q}_i(t)$ [L^3/T] is the previous combined hydrograph flow that resulted in a shift from either increasing or decreasing subsurface flow; α ($0 < \alpha < 1$) is the threshold factor that identifies the flow on the recession limb of the response hydrograph where flow is defined by the recession model (i.e., where $Q_{ss,i}(t)$ shifts from recession to increasing); and k ($0 < k < 1$) is the exponential decay constant. The subsurface response model, Equation (3), has two expressions, with the left and right most relationships defining increasing and decreasing $Q_{ss,i}(t)$, respectively. The quantity $\hat{Q}_i(t)$ in Equation (3)is continually reset as $Q_{s,i}(t)$ increases and decreases (i.e., when the maximum value from Equation 3 switches between the expression for increasing and decreasing flow). Within the study watershed, it is assumed that the two primary sources of subsurface runoff are shallow soil and ground water flow. To approximate these two conditions in the model, subareas classified as having steep shallow soil flow have a more rapid decay, k, and larger threshold flow ratio, a, than subareas classified as having ground water flow.

Spatial Data

The primary sources of spatial data used were: topography, drainage networks (i.e., streams and storm sewers), hydrologic soil characteristics, land use, and long term precipitation. Topography was derived from USGS Digital Elevation Models (DEM) with a spatial resolution of 30-meter by 30-meter grid cells. The drainage network is a combination of stream locations (USGS, 1999) and storm drains digitized from county and city drainage maps. The Soil Survey Geographic (SSURGO) Data Base (NRCS, 1995) for Santa Barbara County provides soils data. The SSURGO coverage indicates that the upland areas in this region are generally characterized by thin soils over weathered bedrock with rock outcroppings, while the coastal plain tends to have deeper soils with no known bedrock layer in the upper 2 meters of soil. The current land use for this region was inferred from 1:42,000 scale aerial photographs taken in 1998 and classified based on Anderson Level III classifications (Anderson *et al.*, 1976). For the urbanization analysis, additional land use coverages were 1929, 1986 (developed similarly to the 1998 land use), and 2050 (projected land use based on Candau, 2002). The 1986 and 1998 land use data were used to assess change in land use during the stream gauging period (1989 to 2002). Monthly and annual precipitation contours were obtained from the Parameter Elevation Regressions on Independent Slopes Model (PRISM) (Daly *et al.*, 1994) to evaluate the spatial distribution of rainfall within the watershed.

Spatial patterns of input variables were assigned on a subwatershed basis. The overall watershed shown in Figure 1 was delineated and divided into subareas using a 30-meter DEM, modified to include the known locations of streams and storm drains (Moglen and Beighley, 2000). The delineation follows the rule that water will flow in the direction of the local gradient, making it possible to infer flow directions, flow lengths, slopes, drainage area, and catchment boundaries (O'Callaghan and Mark, 1984; Jenson and Domingue, 1988; Tarboton *et al.*, 1991). Using the inferred drainage network, the watershed was subdivided to isolate drainage areas of approximately 2 km^2. This threshold area resulted in subareas approximately homogeneous in land use, hydrologic soil characteristics, slope, and annual precipitation. Next, modeling variables were calculated from the GIS data and spatially averaged such that a single measure represents an entire subarea.

Temporal Rainfall/Runoff Data

For the period of simulation, 15-minute flow data were obtained for the two USGS stream gauges, and precipitation data were obtained from eight gauges operated by Santa Barbara County Flood Control (Figure 1). The rainfall gauges provide daily totals and limited intensity data. Only the intensity data from Gauge 228 were available for the complete simulation period and were converted to a 15-minute time series. To incorporate the effects of orographic precipitation at the subarea scale, four additional 15-minute time series were developed to represent different elevation zones: $E_i \leq 100$ m; 100 m $< E_i \leq 300$ m; 300 m $< E_i \leq 600$ m; and $E_i > 600$ m, where E_i is the average elevation in subarea *i*. The values for the various elevation zones were determined based on the relationship between total precipitation and gauge elevation for the entire 14-year period (Figure 4). The linear nature of the *P-E* relationship shown in Figure 4 is also consistent with the PRISM contours for this region (Daly *et al.*, 1994). Subarea precipitation, $P_i(t)$ [L/T], was determined by

$$P_i(t) = P_g(t)\left(\bar{P}_k / \bar{P}_g\right) \tag{4}$$

where $P_g(t)$ [L/T] is the 15-minute time series from Gauge 228; $\bar{P}_g$ [L] is the total precipitation from the 15-minute data for Gauge 228 for the 14-year period; and $\bar{P}_k$ [L] is the average total precipitation from the daily data for all gauges within the elevation zone corresponding to E_i [L] for the 14-year period.

Model Parameterization

The parameterization of the HEC-HMS model was done in two steps. First, the watershed was subdivided as described previously, and GIS algorithms described by Olivera (2001) were used to develop the HEC-HMS basin model. Second, the basin model was linked to the spatial database using Visual Basic, and initial parameter values were estimated using various guidelines. Parameter guidelines were based on assumed subsurface flow conditions and land use. Subareas were classified as having either: (1) steep shallow soils, average ground slope greater than or equal to 25 percent and a known bedrock layer within the upper 0.5 meters of soils or (2) deeper soils on moderate slopes (Figure 1).

The loss model parameters for subareas classified as steep shallow soils were initially set to the values shown in Table 4. The maximum storage capacity values ($S_{m,i}$) in Table 4 are based on the average depth of soil above bedrock and porosity as reported from SSURGO, and the constant loss rates, I_i, were estimated using soil texture from SSURGO and conversion tables from Rawls *et al.* (1983). For subareas classified as deeper soils on moderate slopes, maximum storage values were estimated based on land use and typical surface losses given by Viessman *et*

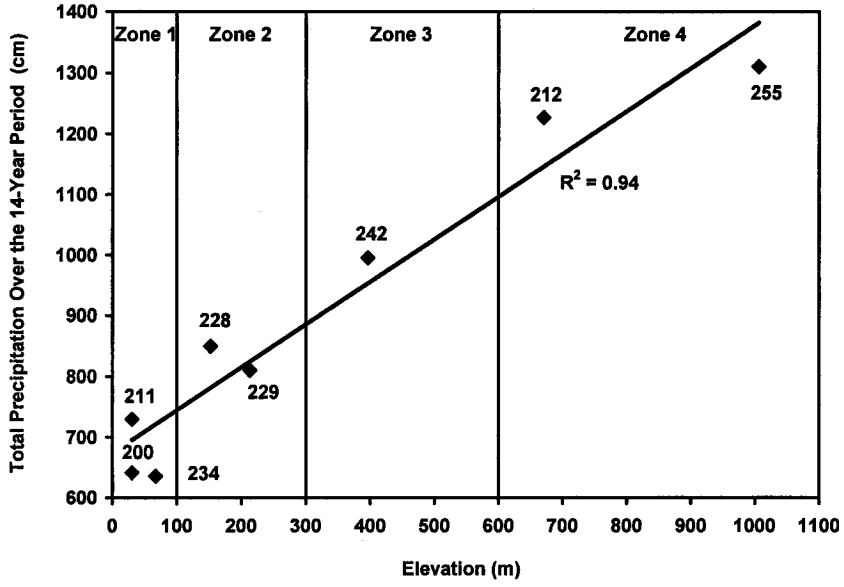

Figure 4. Relationship Between Total Precipitation and Elevation for the Water Years 1989 Through 2002 for the Atascadero Creek Watershed With the Four Elevation Zones Separated by Vertical Lines. Refer to Figure 1 for gauge locations corresponding to the gauge numbers associated with each data point.

TABLE 4. Initial and Calibrated Loss Model Parameters. S_m is the maximum storage capacity, I is the constant loss rate, and L is the monthly storage recovery rate, which is the same for all months unless otherwise specified.

	Initial Parameters			Calibrated Parameter		
Subarea Classification	S_m (cm)	I (cm/hr)	L (cm/day)	Sm (cm)	I (cm/hr)	L (cm/day)
Steep Shallow Soil Flow	3.7 to 11.8	0.3 to 0.9	2.5	10.2	1.3	2.5 (February = 1.3, March = 0.6)
Ground Water Flow	0.6 to 1.9	0.5 to 1.8	2.5	1.3	1.5	2.5 (February = 1.3, March = 0.6)

al. (1977), and constant loss rates were also approximated using soil texture and conversion tables. The storage recovery rates, $L_i(t)$, were set to 2.5 cm/day for all months and all subareas. The percentage of impervious area in each subarea was estimated from the land use coverages using lookup tables that relate land use classification to imperviousness (NRCS, 1986). The lookup tables were validated by sampling a few locations for imperviousness with high resolution land use (parcels) data.

The routing parameters were estimated from the inferred drainage network (Table 3). Overland and channel flow parameters were estimated from the topographic, channel cross sections, and land use data. Channels were assigned as trapezoidal with top widths increasing from 3 m in first order streams to 10 m for larger streams based on field observation; channel side slopes were estimated as 45 degrees for natural channels and as vertical for engineered channels in urbanized areas (i.e., subareas more than 15 percent impervious). Overland flow roughness coefficients were estimated using lookup tables relating land use to roughness (NRCS, 1986), with shrub/brush, agricultural, and urban land uses having roughness, N, values of 0.6, 0.4, and 0.2, respectively. Channel roughness coefficients (Manning's n) were estimated at 0.06, 0.04, and 0.025 for mountainous, coastal plain agricultural, and coastal plain urban regions, respectively (Chow, 1959; Barnes, 1967).

Subsurface flow parameters for subareas designated as steep shallow soils were estimated from observed hydrographs from the tributary gauge, USGS 11119940. Ground water flow parameters were estimated from outlet gauge, USGS 11120000. Parameters α and k were set to 20 percent and 0.05 and 10 percent and 0.10 for shallow soil and ground water flow, respectively, highlighting the differences between the two classifications with shallow soil flow occurring sooner and having a steeper decay.

MODEL CALIBRATION AND VERIFICATION

The HEC-HMS model parameters were calibrated for the period October 1, 1988, through September 30, 1995, and verified for the period October 1, 1995, through September 30, 2002, using 1998 land use conditions. Table 5 shows that the 1998 land use conditions are representative of the entire period, with essentially no change in land use between 1986 and 1998. The intent of model calibration and verification is to demonstrate that the modeling approach and spatial/temporal distribution of rainfall adequately reproduce streamflow for the 14-year simulation period such that the effects of urbanization and varying climatic conditions can be investigated.

TABLE 5. Percent of Land Use in the Atascadero Creek Watershed for 1929, 1986, 1998, and 2050 Conditions.

Year or Period	Urban	Shrub/ Brush	Agricultural	Imperviousness
1929	8.0	63.8	28.2	4.0
1986	37.8	54.2	8.0	17.2
1998	38.4	50.5	11.1	17.4
2050	52.2	47.0	0.9	24.4

The calibration period (1989 to 1995) was selected as representative of the overall study period with a mix of El Niño, La Niña, and normal climatic conditions (Table 2). While the watershed contains 31 subareas (Figure 1), the calibration process focused on the two subarea classifications, and a single set of $S_{m,i}$ and I_i values was used for each classification because of the similarity of parameter values within each group (Table 4). For example, the maximum storage capacity in all subareas classified as steep shallow soils was adjusted to 8.5 cm (average value with range 3.7 to 11.8 cm), and based on model performance, $S_{m,i}$ was increased or decreased uniformly in all shallow soil subareas.

During the calibration process, model performance was assessed on the accuracy of peak discharge and runoff estimates using relative error, RE, (%)

$$RE = \frac{x_o - x_s}{x_o} \ 100\% \qquad (5)$$

and absolute error, AE, (m^3/s or cm)

$$AE = |x_o - x_s| \quad (6)$$

where x_o is the measured value of either peak discharge or runoff depth and x_s is the simulated value. The peak discharges used for the error analysis were from events that produced peak flows exceeding approximately 22 and 3.0 m^3/s for Gauges 11120000 and 11119940, respectively. Fourteen peak discharges from each gauge exceeded these threshold values for both the calibration and validation periods (approximately two events per year for each gauge).

To minimize model error (i.e., RE and AE in peak discharges and runoff depth), parameter adjustment focused on two issues: (1) maximum storage capacity and loss rates and (2) storage recovery rates. The maximum storage capacity, $S_{m,i}$, and rate at which rainfall enters the storage reservoir, I_i, most notably affected model performance in dry conditions, when it can be assumed that the initial storage capacity, $S_i(t)$, was near zero (i.e., storage reservoir was empty). The storage recovery rate, $L_i(t)$, affected model performance during a series of storms. Table 4 provides the calibrated model parameters. While the calibrated storage and infiltration parameters are similar to their initial estimates, the adjustments generally reduced predicted peak discharge and runoff depth. The calibrated recovery loss rate, $L_i(t)$, was reduced to 1.3 and 0.6 for February and March, respectively, to account for increasing saturation during the rainy season. After calibration, the error in Q_p for Gauges 11120000 and 11119940 was 10 percent (12.4 m^3/s) and 15 percent (6.2 m^3/s), respectively, and the error in annual runoff was -0.2 percent (-0.2 cm) and 19.4 percent (19.1 cm), respectively (Table 6).

While the error in runoff at Gauge 11119940 might be considered excessive, a portion of the model error is likely due to gauging error. Along the Santa Barbara coast, gauging errors and/or missing data are a common problem primarily due to the rapid hydrograph response and extended dry periods. While these issues are generally resolved or noted in the daily data provided by the USGS, our work required high resolution, provisional 15-minute data. For example, the data quality flags provided by the USGS indicate that the daily data from Gauges 11120000 and 11119940 are adjusted or estimated about 3 and 7 percent of the time, respectively. In the case of Gauge 11119940, the data appears reasonable for the rising limb and peak discharges based on comparisons to other gauges in the region. However, the gauge occasionally overestimates falling limb discharges. For example, in three days following a peak discharge in January 1995, Gauge 11120000 measured 0.3 cm of runoff, while Gauge 11119400, 32 percent of Gauge 11120000's drainage area, measured 1.7 cm. In this three-day period, the discharge from Gauge 11120000 decreased from 1.4 to 0.3 m^3/s, while the discharge from Gauge 11119940 decreased from 1.4 to 0.7 m^3/s. Thus, it is likely that Gauge 1119940 over-estimated discharge, which is consistent with the model error shown in Table 6. Given the difficulty in detecting and resolving these potential errors, the available data were used, and the model error for runoff at Gauge 11119940 was accepted.

To validate the calibrated model parameters, streamflow was simulated for the period October 1, 1995 through September 30, 2002. For peak discharge, the model performance for the validation period is similar to the calibration period; for runoff depth, the model performance is less favorable but

TABLE 6. Model Calibration and Validation Statistics for USGS Gauges 11120000 and 11119940. The mean, minimum, and maximum peak discharges, Q_p, and runoff are from the measured data and the relative error, RE, and absolute error, AE, represent average errors for individual peak discharges and annual runoff from each water year simulated.

	Calibration (WY 1989 to 1995)		Validation (WY 1996 to 2002)	
Summary Statistic	**11120000**	**11119940**	**11120000**	**11119940**
Mean Q_p (m^3/s)	81.7	31.4	59.1	15.6
Min Q_p (m^3/s)	30.8	6.7	22.6	3.0
Max Q_p (m^3/s)	289.7	130.1	270.6	58.4
RE, Q_p (percent)	10.4	15.2	12.5	12.2
AE, Q_p (m^3/s)	12.4	6.2	15.5	6.1
Runoff (cm)	100.9	98.2	99.4	94.4
RE, Runoff (percent)	-0.2	19.4	13.9	27.2
Error, Runoff (cm)	-0.2	19.1	13.8	25.7

still reasonable (Table 6). The generally positive calibration and validation results show that the model can be used to simulate streamflow from varying land uses and climatic conditions. While the probable differences between measured and inferred rainfall, stream gauge error, and simplified complexities of the system imply a certain level of modeling uncertainty, the intent of the calibration and validation process was not to match each hydrograph exactly but to assess whether broad trends in the hydrologic effects of land use change can be predicted.

ALTERNATIVE LAND USE SCENARIOS

To assess the impacts of existing and future urbanization on the annual and 14-year distributions of streamflow, two alternative land use scenarios were modeled: predevelopment in 1929 and projected development in 2050 (Figure 5 and Table 5). As described in Candau (2002), the projected 2050 land use coverage was determined using the SLEUTH model, a modified cellular automaton urban growth model named for the input data used to initialize the model: Slope, Land Use, Exclusion, Urban, Transportation, and Hillshade and described by Clarke and Hoppen (1997). The SLEUTH model has been successfully applied in various locations in the United States, Mexico, and Europe. The model incorporates growth trends, topography, protected lands (e.g., National Forest lands), transportation networks, and existing land use. For the Santa Barbara region, the model was calibrated using seven historical land use coverages: 1929, 1943, 1956, 1967, 1976, 1986 and 1998.

Based on Candau (2002), urbanization is projected to increase by 14 percent between 1998 and 2050. However, assessing the quality of future land use projections is difficult because data are not available for comparison and estimates are often driven by historical growth trends. To assess the Santa Barbara forecast, population estimates and current land use planning concepts were investigated. Based on population growth forecasts for the next 30 years, 104,000 (SBCPD, 2000) to 247,000 people (CADOF, 2001), Santa Barbara County faces a significant demand for additional housing. Using the current growth plan for Santa Barbara County – increasing the density of residential development and urban infill (i.e., redeveloping parcels within the urban extent) – the Santa Barbara-Goleta area will buildout the existing urban footprint in less than eight years (Candau, 2002). The shift towards increasing density to limit urban growth is evident over the past 10 years, which showed only a minor increase in the urban footprint. Recall that there was essentially no change in land use between 1986 and 1998 (Table 5). Growth was also limited in the 1990s due to a water moratorium on new construction as a result of a significant drought during the late 1980s and early 1990s. Now that the South Coast is part of the state water project (i.e., additional water supply), and few parcels are available for urban infill and a significant demand for additional housing is likely, it is projected that the urban footprint will rapidly expand over the next 30 years (SBCPD, 2000). Given that both the county and state predict significant increases in populations over the next 30 years and that the mountains and ocean limit available land for future development, the 2050 projections by Candau (2002) shown in Figure 5 are reasonable.

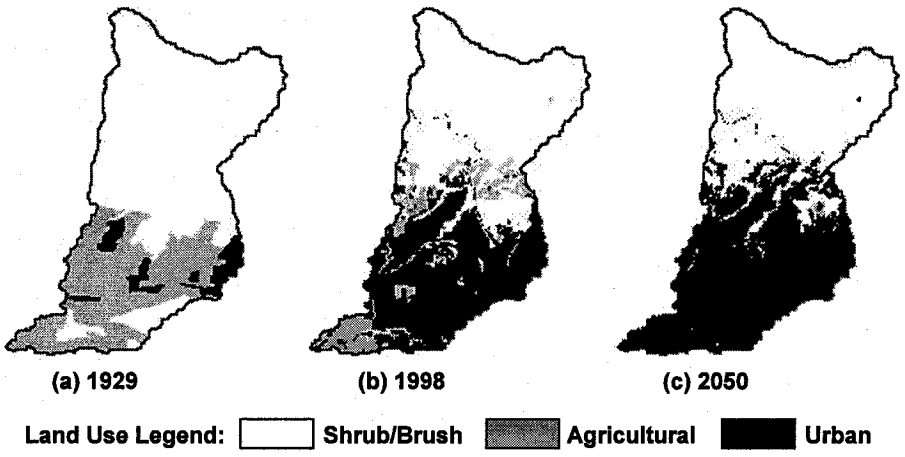

Figure 5. Land Use Distributions From (a) 1929, (b) 1998, and (c) 2050 (projected) for the Atascadero Creek Watershed.

Figure 5 shows that the coastal plain is completely built out and the urban footprint expands into the foothills region, where agricultural lands are replaced with urban development.

In terms of growth rates, the projected 2050 development shows less increase in urban land uses (i.e., 14 percent urban, 7 percent impervious) relative to the increase from 1929 to 1998 (i.e., 30 percent urban, 13 percent impervious). However, unlike the urbanization that took place from 1929 to 1998, future development is expected to spread up the mountain side, increasing the sensitivity of the watershed response as high elevations receive more rainfall than the coastal plain. Generally, the largest flood events, which account for the major portion of total annual runoff, derive from the upper, rainier areas of the watershed. Urbanization also decreases travel times, which, when combined with increased runoff from impervious areas, increases peak discharges at the watershed outlet. While historical daily streamflow data are available since 1940 to study the influence of urbanization on runoff volume in the Atascadero Creek watershed, it is difficult to infer the potential impacts of future development from the past because of orographic rainfall enhancement and the predicted location of future urbanization. Using the approach discussed herein, we quantify the effects of both the magnitude of land use change and its spatial distribution within the watershed on the annual and 14-year distributions of streamflow, annual peak discharges, and runoff. To account for hydrologic impacts of land use change, surface and channel roughness coefficients, channel shape, and impervious area within each subarea were modified based on the alternative subarea land use conditions using the assumptions previously mentioned in the Model Parameterization section.

RESULTS

For consistency, the previously validated simulated discharge series (1989 to 2002) for the 1998 land use conditions were used for comparison with the two alternate land use scenarios. Table 7 provides summary measures for the period of simulation for all three land use scenarios. For each land use scenario, Figure 6 shows the average annual distribution of streamflow for El Niño, La Niña, and normal years divided by the total 14-year discharge associated with the corresponding land use conditions (i.e., Figure 6 cannot be used to assess the magnitude of streamflow from the various land use scenarios).

The 1929, 1998, and 2050 land use scenarios resulted in an average annual maximum discharge of 65, 87, and 110 m^3/s with a range between years from 2 to 214, 10 to 266, and 19 to 305 m^3/s, respectively (Table 7). Similarly, the 1929, 1998, and 2050 scenarios resulted in an average annual runoff of 7, 15, and

TABLE 7. Simulation Results for 1929, 1998, and 2050 Land Use for the Atascadero Creek Watershed, Q_p is annual peak discharge, Q is annual runoff, and 1-day and 10-day percentages represent the fraction of the annual flow released in the maximum 1 day and 10 days of flow during the water year.

	1929 Land Use Conditions				1998 Land Use Conditions				2050 Land Use Conditions			
Water Year	Q_p (m^3/s)	Q (cm)	1 Day (percent)	10 Day (percent)	Q_p (m^3/s)	Q (cm)	1 Day (percent)	10 Day (percent)	Q_p (m^3/s)	Q (cm)	1 Day (percent)	10 Day (percent)
1989	2	0.9	25	80	13	3.6	29	84	26	6.1	30	84
1990	6	0.8	36	87	18	2.9	38	91	35	4.8	39	92
1991	49	6.5	44	95	69	12.7	33	92	94	18.0	30	91
1992	165	9.7	59	91	207	18.6	38	80	251	26.8	32	76
1993	66	8.5	37	84	87	19.5	25	73	113	30.4	23	71
1994	20	2.4	35	81	30	7.0	29	77	43	12.2	29	76
1995	214	30.3	52	90	266	50.1	38	77	305	67.5	32	72
1996	35	3.4	37	82	52	11.2	23	74	68	17.5	22	72
1997	6	2.3	28	81	19	8.2	24	79	35	13.7	24	79
1998	116	18.3	37	91	150	30.4	30	83	174	40.8	28	81
1999	2	1.0	22	68	10	4.3	26	73	19	7.3	26	74
2000	37	4.0	32	79	53	11.3	23	74	72	17.6	22	73
2001	181	10.3	50	90	216	23.1	30	78	245	33.4	26	76
2002	9	1.1	33	79	28	4.5	28	80	55	7.9	27	80

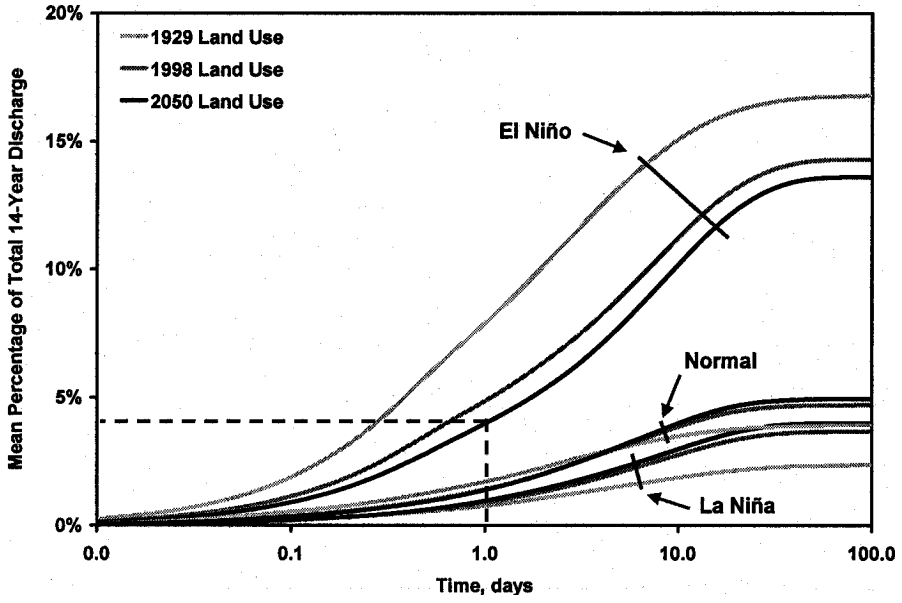

Figure 6. Mean Percentage of Annual Discharge for 1929, 1998, and 2050 Land Use Conditions Exceeded in a Given Time Period for La Niña, El Niño, and Normal Years. The distributions for each water year were determined by cumulating the 15-minute discharges ranked in decreasing order and dividing by the total 14-year discharge associated with the corresponding land use conditions.

22 cm ranging from 1 to 30, 3 to 50, and 5 to 67 cm, respectively. In all cases, annual peak discharges and runoff increased with increasing urbanization. Comparing the two periods of urbanization (i.e., 1929 to 1998 and 1998 to 2050), the average increase in annual peak discharges and runoff depths from 1929 to 1998 (22.2 m^3/s and 7.7 cm) was similar to the increase from 1998 to 2050 (22.5 m^3/s and 6.9 cm). For the entire period of urbanization (1929 to 2050), the average increase in annual maximum discharges and runoff depths was approximately 45 m^3/s (300 percent) and 15 cm (350 percent), respectively.

Combining the effects of land use change and varied climate conditions, the average annual maximum discharges from the four El Niño years (1992, 1993, 1995, and 1998) and the four La Niña years (1989, 1996, 1999, and 2000) for the 1929, 1998, and 2050 land use scenarios were 140, 178, and 211 m^3/s (El Niño) and 19, 32, and 46 m^3/s (La Niña), respectively. The average annual runoff from El Niño years and La Niña years for the 1929, 1998, and 2050 land use scenarios were 17, 30, and 41 cm and 2, 8, and 12 cm, respectively.

Changes in the annual flow distributions due to land use alterations were evident for the various climatic conditions. In El Niño years, the percentage of annual runoff occurring in either the maximum one or 10 days of flow was greater for the 1929 land use conditions compared with 1998 or 2050 (Table 7). In La Niña and normal years, the percentage of annual discharge occurring in either one or 10 days was generally smallest in 1929. Regardless of land use and climatic conditions, the annual flow distributions were significantly skewed with the maximum one or 10 days of streamflow accounting for more than 20 and 70 percent, respectively, of the annual runoff.

Figure 6 shows the effect of climatic conditions on inter-annual streamflow variability. El Niño years dominate the 14-year period, with the maximum 10 days of flow from an average El Niño year accounting for 15, 11, and 10 percent of the total 14-year discharge for 1929, 1998, and 2050 conditions, respectively, compared with 2, 3, and 3 percent for an average La Niña year. Figure 6 also illustrates only a marginal difference between La Niña and normal conditions over the period of simulation.

DISCUSSION

The results show that urbanization increases peak discharges and annual runoff, but the magnitudes of these changes were not proportional to increases in urbanization because of how urban development spreads upslope from the coastal plain into the higher rainfall zone. Thus, the effects of urbanization were compounded by orographic rainfall and decreased travel times. For example, the increase in urbanization from 1928 to 1998 was 30 percent (38.4 percent

in 1998 to 8.0 percent in 1929 = 30.4 percent), while the increase from 1998 to 2050 was only 13.7 percent (i.e., less than half as large). However, the average change in annual peak discharges and runoff depths were similar (approximately 22 m^3/s and 7 cm).

The effects of climatic and land use conditions on annual maximum discharge and runoff were significant. For the nonurban scenario (i.e., 1929), the average annual peak discharge and runoff depth from the four El Niño years (140 m^3/s and 17 cm) were 7.4 and 7.1 times, respectively, greater than from the La Niña years (19 m^3/s and 2 cm). For the urban scenario (i.e., 2050), the average annual peak discharge and runoff depth from the four El Niño years (211 m^3/s and 41 cm) were 4.5 and 3.4 times, respectively, greater than from the La Niña years (46 m^3/s and 12 cm). Regardless of land use, the highly varied climatic conditions result in dramatic inter-annual variability in streamflow from the Atascadero Creek watershed.

While urbanization increases peak flow and runoff, the variability of the rainfall/runoff response was largest in a nonurban system because urbanization increases the percentage of impervious surfaces. For smaller events, near the threshold of runoff, increased imperviousness resulted in significantly more runoff. For larger storms, the effect of increased imperviousness was minimal because a larger fraction of the watershed "saturates" relatively early during the event, essentially diminishing the effects of initial storage capacity provided by nonurban lands. For a given increase in impervious area, the percent increase in peak discharge and runoff volume generally decreases with increasing rainfall magnitude. For example, comparing results from the 1929 and 2050 scenarios shows that the minimum annual peak discharges and runoff depths increased by 930 and 510 percent, respectively, while the maximum annual peak discharges and runoff depths increased by only 43 and 120 percent, respectively. Thus, while urbanization increases peak discharges and runoff volume, it tends to reduce the range of streamflow variability. This point is illustrated in Figure 6, which shows that the 1929 scenario produces the greatest difference between El Niño and La Niña conditions; the difference between these two extreme climatic conditions decreases with increasing urbanization.

It is important to note the dominance of only a few large events regardless of land use. For the 1929, 1998 and 2050 conditions, the percentage of annual runoff occurring in the maximum one day of flow ranges from 22 to 52, 23 to 38, and 22 to 39 percent, respectively, while the percentage of runoff from the 14-year period occurring in one day ranges from 0 to 16, 1 to 9, and 1 to 7 percent, respectively. For the Atascadero Creek watershed, runoff and the associated products (nutrients, sediments, etc.) are exported to the ocean in short duration, high magnitude pulses. The variability and magnitude of the pulsed response are directly related to climate conditions, with urbanization increasing the magnitude and decreasing the variability. The degree to which the streamflow signal maybe altered is a function of how and where the watershed is developed in the future, with increased imperviousness at higher elevations having the greatest impact.

CONCLUSIONS

The HEC-HMS model was calibrated using two USGS stream gauges located within the watershed and inferred rainfall from eight gauges in and around the watershed for the recent 14-year period in the Atascadero Creek watershed located along the southern coast of California. The calibrated model, which was based on 1998 land use conditions, was then adjusted to quantify the streamflow hydrology to be expected from an identical weather series for historical and projected land use scenarios: 1929 and 2050. Simulated streamflow from the three land use scenarios was used to assess the effects of urbanization and climatic conditions (i.e., El Niño and La Niña) on the annual and 14-year period distributions of streamflow, peak discharges, and annual runoff.

As the watershed continues to urbanize, future development is projected to spread upslope from the coastal plain, where the effects of urbanization are compounded by the orographic rainfall and the spatial distribution of development. Thus, continued urbanization will have a greater relative impact on peak discharges and runoff volume than past development. In terms of annual and multiyear streamflow distributions, increasing urbanization results in a less variable rainfall/runoff response because it disproportionately increases runoff from small versus large floods. In all cases, the inter-annual variability in streamflow depended on climatic variations, with El Niño years producing approximately five times as much streamflow as La Niña years. Regardless of land use conditions, the temporal distribution of runoff is dominated by only a few annual events, with the percentage of annual runoff occurring in 24 hours ranging from 22 to 52 percent.

Evaluating the potential impacts of urbanization on streamflow from coastal watersheds in southern California is especially important because of the potential increase in downstream flooding risk and severity and degraded water quality entering the nearshore ecosystem, which is a valuable economic and habitat resource. Understanding and quantifying these impacts will aid land use planners in deciding

how and where to accommodate future housing needs, while providing ecosystem scientists with the altered streamflow signal entering their study systems. In this study, we have shown by how much projected future urbanization in a coastal watershed with a Mediterranean climate will decrease annual and year to year streamflow variability, while increasing the magnitude of peak discharges and annual runoff. These changes in streamflow characteristics result from the combined effects of orographic rainfall, decreased travel times, and the projected spatial development pattern. While one possible scenario is presented, our approach can be used to evaluate other development plans and/or land use projections and assess their potential impacts on the streamflow signal.

ACKNOWLEDGMENTS

This research was conducted as part of the Santa Barbara Channel Long Term Ecological Research Project supported by the National Science Foundation under Cooperative Agreement No. OCE-9982105. We acknowledge the Mesoscale Effects of Climate and Land-Cover Change on River-Basin Hydrology in Amazonia Project supported by the National Aeronautics and Space Administration under Cooperative Agreement No. NAG5-8396 for providing added research focus. We also thank the Urban Change-Integrated Modeling Environment Project supported by the National Science Foundation under Cooperative Agreement No. OCE-9817761, the Santa Barbara County Public Works Department, and the USGS for their generous sharing of data.

LITERATURE CITED

Anderson, J. R., E. E. Hardy, J. T. Roach, and R. E. Witmer, 1976. A Land Use and Land Cover Classification System for Use With Remote Sensor Data. U.S. Geological Survey, Professional Paper 964, Reston, Virginia, 28 pp.

Barnes, H. H., 1967. Roughness Characteristics of Natural Channels. U.S. Geological Survey, Water Supply Paper 1849, Reston, Virginia, 213 pp.

Beighley, R. E. and G. E Moglen, 2002. Trend Assessment in Rainfall-Runoff Behavior in Urbanizing Watersheds. ASCE Journal of Hydrologic Engineering 7(1):27-34.

CADOF (California Department of Finance), 2001. Interim County Population Projections. Sacramento, California, June 2001. *Available at* http://www.dof.ca.gen/html/demograp/P1.doc. *Accessed on* June 18, 2003.

Candau, J., 2002. Temporal Calibration Sensitivity of the SLEUTH Urban Growth Model, Dissertation, UC No. 002401308, Department of Geography, University of California, Santa Barbara, California.

Chow, V. T., 1959. Open Channel Hydraulic. McGraw-Hill, New York, New York.

Clarke, K. C. and S. Hoppen, 1997. A Self-Modifying Cellular Automaton Model of Historical Urbanization in the San Francisco Bay Area. Environment and Planning A 24:247-261.

Daly, C., R. P. Neilson, and D. L. Phillips, 1994. A Statistical-Topographic Model for Mapping Climatological Precipitation Over Mountainous Terrain. Journal of Applied Meteorology 33:140-158.

Field, C. B., G. C. Daily, F. W. Davis, S. Gains, P. A. Matson, J. Melack, and N. L. Miller, 1999. Confronting Climate Change in California: Ecological Impacts on the Golden State. Union of Concerned Scientists, Cambridge, Massachusetts, and Ecological Society of America, Washington, D.C., 62 pp.

Jensen, S. K. and J. O. Domingue, 1988. Extracting Topographic Structure From Digital Elevation Data for Geographic System Analysis. Photogrammetric Engineering and Remote Sensing 54(11):1593-1600.

Kim, J., T. K. Kim, R. W. Arritt, and N. L. Miller, 2002. Impacts of Increased Atmospheric CO_2 on the Hydroclimate of the Western United States, Journal of Climate 14(14):1926-1941.

McCarthy, J. J., O. F. Canziani, N. A. Leary, D. J. Dokken, and K. S. White (Editors), 2001. Climate Change 2001: Impacts, Adaptation and Vulnerability. Contribution of Working Group II to the Third Assessment Report of the Intergovernmental Panel on Climate Change (IPCC). Cambridge, United Kingdom; Cambridge University Press, New York, New York, 1,032 pp.

Moglen, G. E. and R. E. Beighley, 2000. Using GIS to Determine Extent of Gauged Streams in a Region. ASCE Journal of Hydrologic Engineering 5(2):190-196.

Monteverdi, J. and J. Null, 1997. El Niño and California Rainfall. National Oceanic and Atmospheric Administration, Western Region Technical Attachment No. 97-37.

NOAA (National Oceanic and Atmospheric Administration), 2001. Sulphur Mountain Doppler Radar: A Performance Study. Technical Memorandum NWS WR-267,U.S. Dept. of Commerce, NOAA, National Weather Service, Los Angeles Weather Service, Oxnard, California.

NRCS (National Resources Conservation Service), 1995. Soil Survey Geographic (SSURGO) Data Base. Data User Information. U.S. Department of Agriculture, National Resources Conservation Service, National Soil Survey Center, Miscellaneous Publication Number 1527.

NRCS (Natural Resources Conservation Service), 1986. Urban Hydrology for Small Watersheds. Technical Release 55, Washington, D.C.

O'Callaghan, J. F. and D. M. Mark, 1984. The Extraction of Drainage Networks From Digital Elevation Data. Computer Vision, Graphics and Image Processing 28:323-344.

Olivera, F., 2001. Extracting Hydrologic Information From Spatial Data for HMS Modeling. ASCE Journal of Hydrologic Engineering 6(6):524-530.

Pinol, J., K. Beven, and J. Freer, 1997. Modelling the Hydrologic Response of Mediterranean Catchments, Prades, Catalonia. The Use of Distributed Models as Aids to Hypothesis Formulation. Hydrologic Processes 11:1287-1306.

Rawls, W. J., D. L. Brakensiek, and N. Miller, 1983. Green-Ampt Infiltration Parameters From Soils Data. ASCE Journal of Hydraulic Engineering 109(1):62-70.

Ribolzi, O., P. Andrieux, V. Valles, R. Bouzigues, T. Bariac, and M. Voltz, 2000. Contribution of Groundwater and Overland Flows to Storm Flow Generation in a Cultivated Mediterranean Catchment. Quantification by Natural Chemical Tracing. Journal of Hydrology 233:242-257.

SBCPD (Santa Barbara County Planning and Development), 2000. Santa Barbara County 2030 Land and Population: The Potential Effects of Population Growth on Urban and Rural Lands. Santa Barbara County, Santa Barbara, California.

Smith, C. A. and P. Sardeshmukh, 2000. The Effect of ENSO on the Intraseasonal Variance of Surface Temperature in Winter. International Journal of Climatology 20:1543-1557.

Tarboton, D. G., R. L. Bras, and I. Rodriguez-Iturbe, 1991. On the Extraction of Channel Networks From Digital Elevation Data. Hydrological Processes 5:81-100.

USACE (U.S. Army Corps of Engineers), 2000. HEC-HMS Technical Reference Manual. Hydrologic Engineering Center, Davis, California.

USGS (U.S. Geological Survey), 1999. The National Hydrography Dataset. U.S. Geological Survey Fact Sheet 106-99, Reston, Virginia.

Viessman W., J. W. Knapp, G. L. Lewis, and T. E. Harbaugh, 1977. Introduction to Hydrology. Harper and Row, New York, New York.